Search for single production of vectorlike *B*-quarks at the LHC*

Jin-Zhong Han(韩金钟)[1†] Yao-Bei Liu(刘要北)[2‡] Lu Xing(邢璐)[1] Shuai Xu(徐帅)[1§]

[1]School of Physics and Telecommunications Engineering, Zhoukou Normal University, Zhoukou 466001, China
[2]Henan Institute of Science and Technology, Xinxiang 453003, China

Abstract: New vectorlike quarks have been proposed in many scenarios of new physics beyond the Standard Model, which address the hierarchy problem and may be potentially discovered at the Large Hadron Collider (LHC). Based on a model-independent framework, we propose to search for the vectorlike B-quark (VLQ-B) and focus on resonant production via b-gluon fusion through chromomagnetic interactions. We then explore the possible signals of the VLQ-B through the $B \to tW$ decay mode at the 14 TeV LHC. After a rapid simulation of signal and background events, the 2σ excluded regions and the 5σ discovery reach in the parameter plane of $\kappa_B - M_B$ are obtained at the LHC with an integrated luminosity of 300 (3000) fb^{-1} in the dilepton final states.

Keywords: vector-like quarks, transition chromomagnetic moment, Large Hadron Collider

DOI: 10.1088/1674-1137/ac79ab

I. INTRODUCTION

With the running of the Large Hadron Collider (LHC), the exploration of the heavy resonance, such as additional scalars, new gauge bosons, and charged fermions, has currently reached the TeV-scale. Vectorlike quarks (VLQs) are predicted to provide a dynamical explanation for the large top quark mass in some popular new physics scenarios beyond the standard model (SM) [1], such as little Higgs models [2], composite Higgs models [3], and other new physics theories [4–7]. These new particles do not receive mass through a Yukawa coupling term and thus are not excluded by current searches [8]. Based on their electric charges, such VLQs might appear in $SU(2)$ singlets or multiplets, which can provide rich phenomenology at the current and future high-energy colliders (see, e.g., [9–33]).

Many experimental searches for the VLQs and the constraints on their masses have been conducted. Current searches by the ATLAS and CMS collaborations using LHC Run-II data primarily focus on the quantum chromodynamics (QCD)-induced pair-production modes of VLQs and lead to lower bounds on the vector-like quark masses of approximately 1–1.5 TeV [34–43], depending on the assumed VLQ decay pattern. In this paper, we focus on the VLQ-B with an electric charge of $-1/3$, which is the $SU(2)$ singlet and couple exclusively to third-generation SM quarks. Very recently, the CMS collaboration presented a search for VLQ-B pair production in the fully hadronic final state [43] and excluded the masses up to 1570 and 1450 GeV for 100% $B \to bh$ and 100% $B \to tZ$ cases, respectively.

Given the range of these exclusions, this analysis considers a VLQ-B with a mass greater than 1.3 TeV [44]. For such heavy VLQs, the single production process becomes more important owing to a reduced phase-space and has the added advantage of providing a window to the ultraviolet completion [45–49]. A particularly interesting set of couplings that this may probe are the transition magnetic moments, whether of electroweak nature or chromomagnetic. Simple strategies to probe this were developed in Refs. [50–53]. For transition chromomagnetic moments, an excited bottom quark b^* can be single produced at the LHC via the b-gluon fusion process, $bg \to b^*$ [52, 53]. Searches for such b^* quark have been performed at the LHC by the ATLAS and CMS collaborations at $\sqrt{s} = 7$, 8 and 13 TeV [54–57]. The future high-luminosity phase of the LHC (HL-LHC) is expected to extend the sensitivity in searching for the bounds on the VLQ mass and couplings. In this paper, we focus on the VLQ-B being the $SU(2)$ singlet and coupling exclusively to third-generation SM quarks. We consider the s-channel-resonant production of the VLQ-B at the 14 TeV LHC via the considered chromomagnetic moment and

Received 18 May 2022; Accepted 17 June 2022; Published online 9 August 2022

* Supported by the Foundation of the Key Research Projects in Universities of Henan (22A140019), the Natural Science Foundation of Henan Province (222300420443) and the Project of Innovation and Entrepreneurship Training for College Students in Henan Province (S202110478024)

† E-mail: hanjinzhong@zknu.edu.cn
‡ E-mail: liuyaobei@hist.edu.cn
§ E-mail: shuaixu@cqu.edu.cn

present a careful simulation of the signals and SM backgrounds for the subprocess $bg \to B \to tW^-$ via the dilepton final state.

The remainder of this paper is organized as follows. In Section II, we briefly describe the most general Lagrangian, which is related to the couplings of VLQ-B with the SM particles, and we discuss the decay width in narrow scenarios, the branching ratio, and its single production at the 14 TeV LHC. Section III describes a detector simulation of the signal and the relevant backgrounds at the LHC and its high-luminosity operation phase. We perform a detailed collider analysis to extract the projected sensisitivity of the HL-LHC in probing the parameter space through direct searches in the $B \to tW$ decay channel. Finally, we summarize our results in Section IV.

II. DECAYS AND SINGLE PRODUCTION OF VLQ-B

A. Effective Lagrangian

The general Lagrangian describing the effective interaction of VLQ-B can be expressed as [52]

$$\begin{aligned}\mathcal{L} =& \frac{g_s}{2\Lambda} G_{\mu\nu}\bar{b}\sigma^{\mu\nu}\left(\kappa_L^b P_L + \kappa_R^b P_R\right)B \\ &+ \frac{g_2}{\sqrt{2}} W_\mu^- \bar{t}\gamma^\mu\left(Y_L P_L + Y_R P_R\right)B \\ &+ \frac{g_2}{2c_W} Z_\mu \bar{b}\gamma^\mu\left(F_L P_L + F_R P_R\right)B \\ &+ \frac{m_b}{\upsilon} h\bar{b}\left(y_L P_L + y_R P_R\right)B + \text{H.c.}.\end{aligned} \tag{1}$$

Here, Λ is the cutoff scale, often set to the VLQ-B mass; g_s is the strong coupling constant; $G_{\mu\nu}$ is the field strength tensor of the gluon; g_2 is the $SU(2)_L$ coupling constant; and $\upsilon = 246$ GeV is the electroweak scale. The factors $\kappa_{L,R}^b$, $Y_{L,R}$, $F_{L,R}$, and $y_{L,R}$ parameterize the chirality of the VLQ-B couplings with the different SM particles. When the singlet VLQ-B mixes only with the left-handed bottom quark, we obtain $Y_R\,(F_R) \simeq 0$ and $y_R \simeq \dfrac{M_B}{m_b} y_L$. For simplicity, we consider a benchmark scenario with couplings $Y_L = F_L = y_L = s_L = \upsilon/M_B$. For our objectives, only the magnitude of $\kappa^b = \kappa_{L,R}^b$ is relevant (for more details see Ref. [52] and the references therein), and in the absence of any theoretical knowledge, we consider a phenomenologically guided limit $|\kappa^b| \le 0.5$.

Very recently, the CMS collaboration has searched for a heavy resonance decaying into a top quark and a W boson in the all-hadronic final state [56] and lepton+jets final state [57], respectively. For a benchmark value of the chromomagnetic transition moments ($\kappa^b = 1$), the hypotheses of B quarks with left-handed, right-handed, and vector-like chiralities are excluded at the 95% confidence level for masses below 2.6 (3.0), 2.8 (3.0), and 3.1 (3.2) TeV, respectively. Certainly, for a smaller value of coupling parameter κ^b, such mass limits should be reduced accordingly.

B. Decays width and branching ratio

From Eq. (1), we observe that the VLQ-B decays are dominated by two-body final states, namely $B \to bg$, $B \to tW$, $B \to Zb$, and $B \to hb$. The first of these proceeds through the chromomagnetic moment κ^b. The remaining three are driven by the mixing parameters, and for a very large M_B, they have nearly equal partial widths, which is a consequence of the Goldstone equivalence theorem [58–63]. The partial decay widths of the VLQ-B can be expressed as

$$\Gamma(B \to bZ) = \frac{g_2^2}{128\pi c_W^2}\frac{M_B^3}{M_Z^2}(F_L^2 + F_R^2)(1 - x_Z^2)^2(1 + 2x_Z^2), \tag{2}$$

$$\Gamma(B \to tW^-) = \frac{g_2^2}{64\pi}\frac{M_B^3}{M_W^2}(Y_L^2 + Y_R^2)(1 - x_t^2)^3 + O(x_W^2), \tag{3}$$

$$\Gamma(B \to bh) = \frac{g^2}{128\pi}\frac{M_B^3}{M_W^2}(y_L^2 + y_R^2)(1 - x_h^2)^2, \tag{4}$$

$$\Gamma(B \to bg) = \frac{g_s^2}{12\pi} M_B(\kappa_L^2 + \kappa_R^2). \tag{5}$$

Here, $x_Z = M_Z/M_B$, $x_W = M_W/M_B$, $x_h = M_h/M_B$, and $x_t = M_t/M_B$.

For the fixed coupling parameters $Y_L = F_L = y_L = \upsilon/M_B$, the decay width of the VLQ-B depends on the coupling parameter κ^b and its mass M_B. In Fig. 1, we depict the dependence of width-over-mass ratio Γ_B/M_B on M_B for three values of κ^b. We can observe that, even for

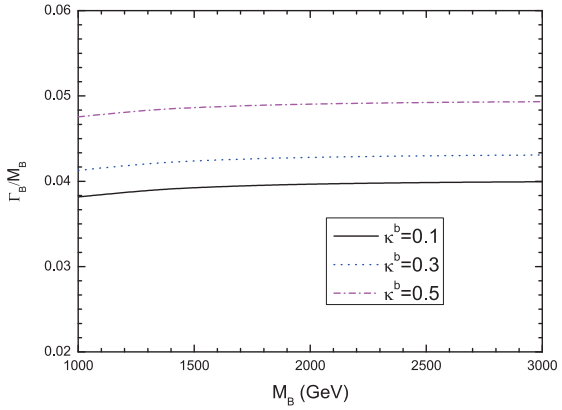

Fig. 1. (color online) Width-over-mass ratio Γ_B/M_B as a function of M_B for different coupling strengths κ^b.

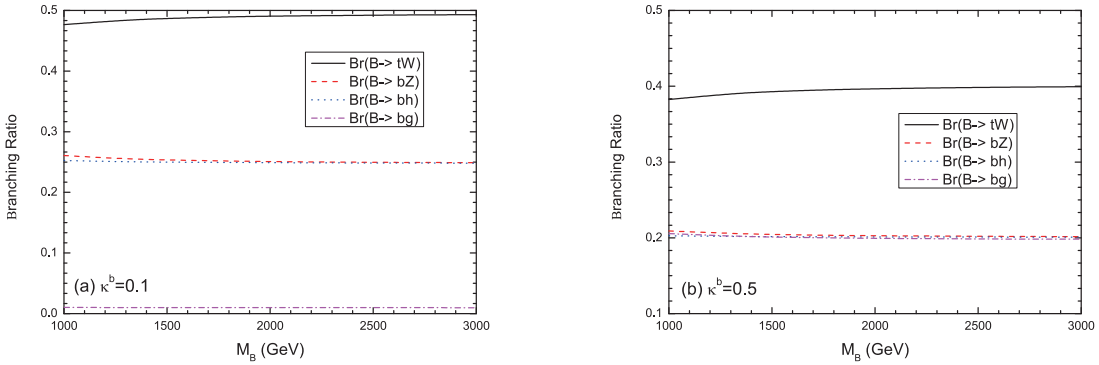

Fig. 2. (color online) Branching ratios for the decay modes Wt, Zb, hb, and bg as functions of M_B for $\kappa^b = 0.1$ (left) and $\kappa^b = 0.5$ (right).

a very large value of κ^b, the ratio $\Gamma_B/M_B \lesssim 0.05$, thereby validating the narrow width approximation.

The branching ratios for these decay channels are plotted as functions of the mass parameter M_B in Fig. 2 for $\kappa^b = 0.1$ and $\kappa^b = 0.5$. We can observe from Fig. 2 that, for $\kappa^b = 0.1$, the branching ratio of the decay mode Wt will increase to approximately 50%, and we obtain $Br(B \to Zb) \simeq Br(B \to hb)$. Certainly, if we take a large value $\kappa^b = 0.5$, the value of the branching ratio $Br(B \to bg)$ will be increased to approximately 20%. This is because for a fixed VLQ-B mass, the partial decay width $\Gamma_{B\to bg}$ is always proportional to $(\kappa^b)^2$.

C. Single production at the LHC

Depending on the strength of the chromomagnetic interactions κ^b, the produced VLQ-B can dominantly decay into a tW system, the Feynman diagram for such resonance VLQ-B production and decay to tW is shown in Fig. 3. The production cross section $\sigma(pp \to B \to tW)$ is plotted in Fig. 4 as a function of the mass M_B for three typical values of the parameter κ^b at the 14 TeV LHC. The leading-order (LO) cross sections are obtained by using MadGraph5-aMC@NLO [64] with NNPDF23L01 parton distribution functions (PDFs) [65] for the renormalization and factorization scales of $\mu_R = \mu_F = \mu_0/2 = M_B$. For $0.1 \le \kappa^b \le 0.5$ and 1000 GeV $< M_B <$ 3000 GeV, the values of the cross section $\sigma(pp \to B \to tW)$ are in the range of $2.1\times10^{-4} \sim 4.4$ pb. For $\kappa^b = 0.3$ and $M_B = 1500$, 1800, 2000 GeV, their values are 0.2, 0.064, 0.032 pb, respectively. Certainly, increasing κ^b would enhance the partial decay width

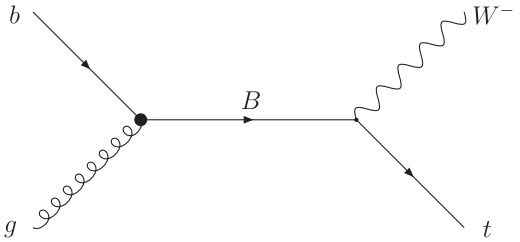

Fig. 3. Feynman diagram for production of a vector-like B quark and decay to a W boson and top quark.

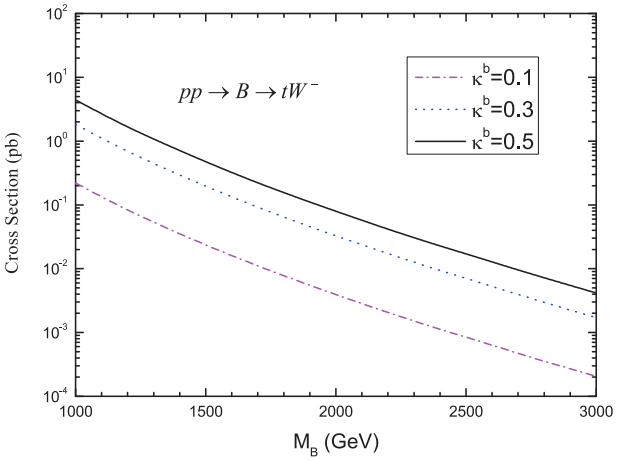

Fig. 4. (color online) Production cross section of the process $pp \to B \to tW$ as a function of M_B for three values of κ^b at the 14 TeV LHC.

$\Gamma(B \to bg)$, thereby suppressing the branching fraction for others.

III. COLLIDER SIMULATION AND ANALYSIS

Next, we explore the discovery potentiality of the singlet VLQ-B through the final states in which both the top quark and W boson originating from the initial VLQ-B decay leptonically.

$$pp \to B \to t(\to b\ell^+\nu)W^-(\to \ell^-\bar{\nu}), \tag{6}$$

where $\ell = e,\mu$. Note that the analysis has included the charge-conjugate process. As a reference point, we set a benchmark value of $\kappa = 0.1$. Analogously, our benchmark points (BPs) in the mass-axis read M_B =1500, 1800, and 2000 GeV. However, later, we will present the reach in the M_B–κ^b plane.

For the above dilepton final states, the main backgrounds are top pair production, the associated tW production, and diboson (WW, WZ, and ZZ) production in association with jets (VV+jets). Here, we do not consider

multijet backgrounds in which jets can fake electrons as they are generally negligible in multilepton analyses [66].

We calculated the leading order (LO) production cross sections and events of signal and backgrounds at parton level using MadGraph5-aMC@NLO. The relevant SM input parameters were obtained from [67]. We then transmitted the parton-level events to Pythia 8 [68] for showering and hadronization. All produced jets were forced to be clustered using FASTJET 3.2 [69] assuming the anti-k_t algorithm with a cone radius of $R = 0.4$ [70]. Detector effects were simulated with Delphes 3.4.2 [71], using the standard HL-LHC detector parameterization shipped with the program. Finally, event analysis was performed using MadAnalysis5 [72]. To consider inclusive QCD contributions, we generated the hard scattering of backgrounds with up to one or two additional jets in the final state, followed by matrix element and parton shower merging with the MLM matching scheme [73]. For the SM backgrounds, we generated LO samples renormalized to the NLO or next-to-NLO (NNLO) cross sections, which are listed in Table 1.

The basic cuts at parton level for the signal and SM backgrounds were set as follows:

$$p_T^{\ell} > 20\,\text{GeV}, \quad p_T^{j} > 25\,\text{GeV}, \quad |\eta_{\ell/j}| < 2.5, \quad \Delta R_{ij} > 0.4 \tag{7}$$

where $\Delta R = \sqrt{\Delta\Phi^2 + \Delta\eta^2}$ is the separation in the rapidity-azimuth plane, and $p_T^{\ell,j}$ are the transverse momentum of leptons and jets, respectively.

For the signal, the final state is required to have exactly two leptons with opposite charges and one central jet. No b-tagging is required because the dominant background from $t\bar{t}$ production also contains b quarks. In Fig. 5, we plot some differential distributions for signals and SM backgrounds after the basic cuts at the 14 TeV

Table 1. K-factors of the leading SM background processes for our analysis.

Process	$t\bar{t}$	tW	VV+jets	Z+jets
K-factor	1.6 [74]	1.35 [75]	1.67 [76]	1.2 [77]

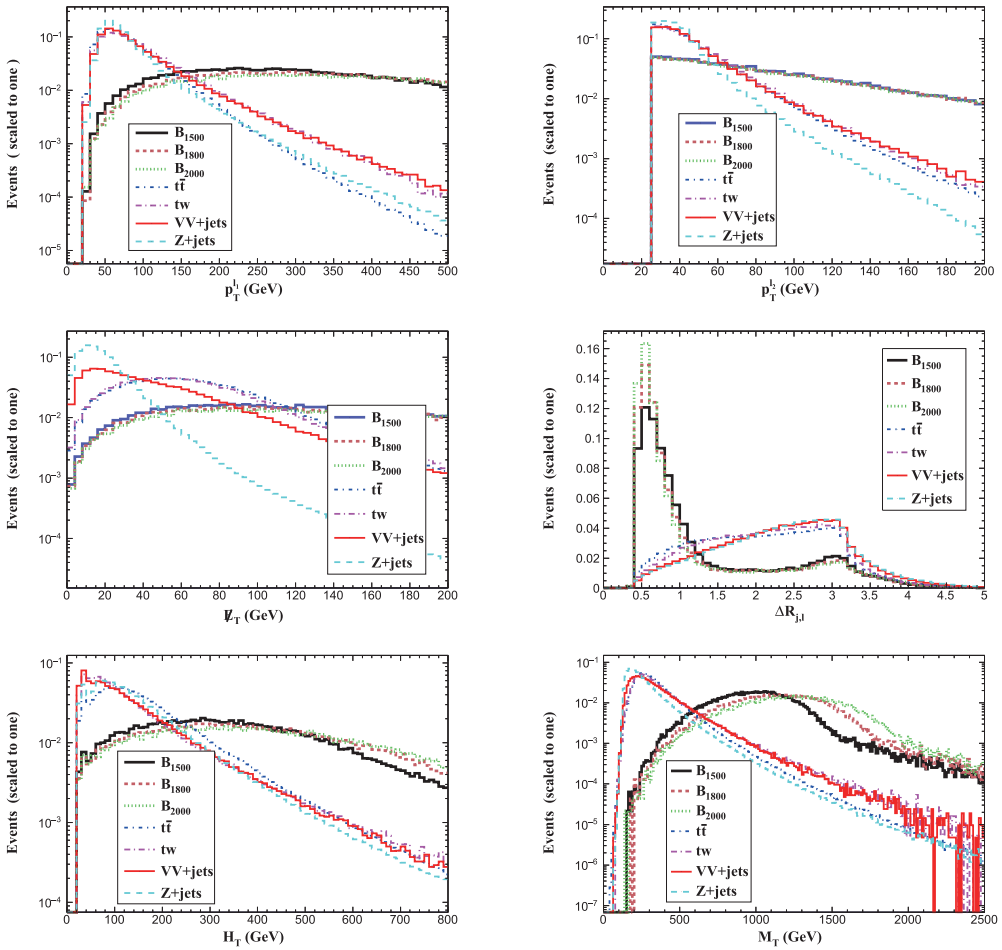

Fig. 5. (color online) Normalized distributions for the signals (with M_B=1500, 1800, and 2000 GeV) and SM backgrounds at the 14 TeV LHC.

LHC, such as the transverse momentum distributions of the leading and sub-leading leptons ($p_T^{\ell_1,\ell_2}$), missing transverse momentum $\not{E}_T^{\rm miss}$, separations $\Delta R_{j,\ell}$, scalar sum of the transverse energy of all final-state jets H_T, and transverse mass distribution $M_T(j\ell_1\ell_2\not{E}_T)$. Here, to reconstruct the VLQ-B mass, we use a cluster transverse mass, defined as [78]

$$M_T^2(j\ell_1\ell_2\not{E}_T) = \Big(\sqrt{p_T^2(j\ell_1\ell_2)+M_{j\ell_1\ell_2}^2}+\not{E}_T\Big)^2 - (\vec{p}_T(j\ell_1\ell_2)+\not{E}_T)^2, \tag{8}$$

where $\vec{p}_T(j\ell_1\ell_2)$ is the total transverse momentum of all visible particles, and $M_{j\ell_1\ell_2}$ is their invariant mass. Owing to the larger mass of VLQ-B, the decay products of VLQ-B are highly boosted. Therefore, the p_T^ℓ peaks of the signals are larger than those of the SM backgrounds, and the angular distance between the jet and the lepton is smaller than that in background process events.

Based on these kinematical distributions, we can impose the following set of cuts to enhance the signal significance.:

- Cut-1: There are exactly two isolated leptons with $p_T^{\ell_1} > 150$ GeV and $p_T^{\ell_2} > 60$ GeV, and at least one jet is required $p_T > 30$ GeV.

- Cut-2: The missing transverse momentum $\not{E}_T^{\rm miss}$ is required to be larger than 60 GeV.

- Cut-3: The separations $\Delta R_{j,\ell}$ and $\Delta R_{\ell_1,\ell_2}$ are required to have $\Delta R_{j,\ell} < 1.0$ and $\Delta R_{\ell_1,\ell_2} > 2.5$.

- Cut-4: The scalar sum of the transverse energy of all final-state jets is required $H_T > 300$ GeV.

- Cut-5: The transverse mass is required $M_T > 1000$ GeV.

We present the cross sections of three typical signals ($M_B = 1500, 1800, 2000$ GeV) and the relevant backgrounds after imposing the cuts in Table 2. We can observe that, at the end of the cut flow, the backgrounds are suppressed very efficiently, and the largest SM background is the $t\bar{t}$ process with the cross section of approximately 1.17 fb.

To analyze the observability, we use the median significance to estimate the expected discovery and exclusion significance [79]:

$$\mathcal{Z}_{\rm disc} = \sqrt{2\left[(s+b)\ln\left(\frac{(s+b)(1+\delta^2 b)}{b+\delta^2 b(s+b)}\right)-\frac{1}{\delta^2}\ln\left(1+\delta^2\frac{s}{1+\delta^2 b}\right)\right]}$$

$$\mathcal{Z}_{\rm excl} = \sqrt{2\left[s-b\ln\left(\frac{b+s+x}{2b}\right)-\frac{1}{\delta^2}\ln\left(\frac{b-s+x}{2b}\right)\right]-(b+s-x)\left(1+\frac{1}{\delta^2 b}\right)}, \tag{9}$$

with

$$x = \sqrt{(s+b)^2-4\delta^2 sb^2/(1+\delta^2 b)}. \tag{10}$$

Here, s and b are the expected events of the signal and total SM background after all cuts, respectively, and δ is the percentage systematic error. To illustrate the effect of systematic uncertainty on the significance, we select three cases: no systematics (δ=0) and two typical systematic uncertainties (δ=5% and δ=10%). In the limit of $\delta \to 0$, these expressions can be simplified as

Table 2. Cut flow of the cross sections (in fb) for the signals and SM backgrounds at the 14 TeV LHC with $\kappa^b = 0.1$ and three typical B quark masses.

Cuts	Signals			Backgrounds			
	1500 GeV	1800 GeV	2000 GeV	$t\bar{t}$	tW	VV+jets	Z+jets
Basic	0.57	0.17	0.077	11700	990	940	41760
Cut-1	0.35	0.11	0.05	520	68	54	1012
Cut-2	0.31	0.094	0.044	302	39	24	136
Cut-3	0.17	0.056	0.026	82	7.8	2.2	0.005
Cut-4	0.10	0.036	0.017	26	1.75	0.54	0.002
Cut-5	0.051	0.024	0.013	1.17	0.26	0.29	0.0002

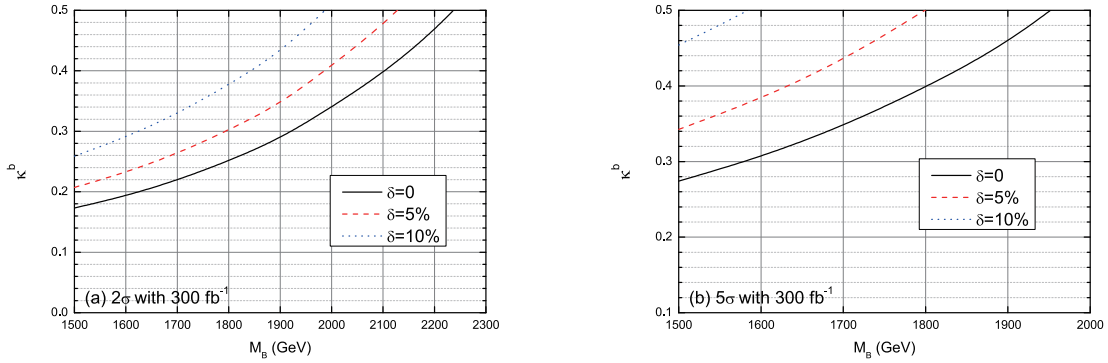

Fig. 6. (color online) Exclusion limit (at 2σ) and discovery prospects (at 5σ) contour plots for the signal in $\kappa^b - M_B$ planes at 14 TeV LHC with an integral luminosity of 300 fb^{-1}.

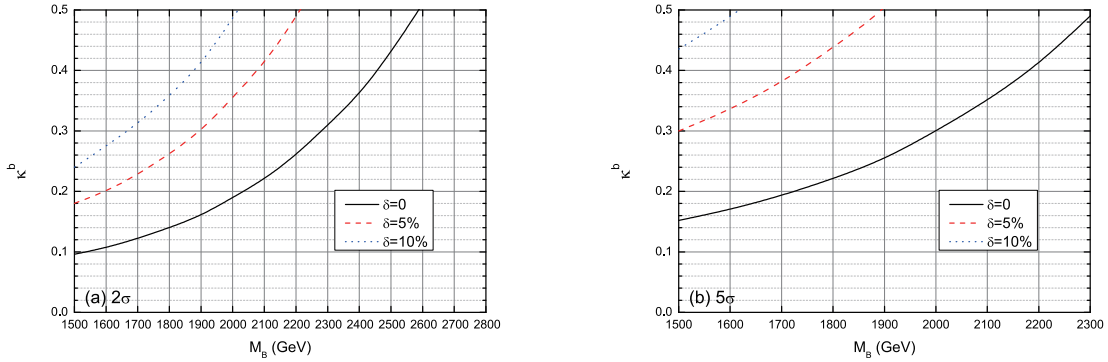

Fig. 7. (color online) Same as Fig. 6, but for the integral luminosity of 3000 fb^{-1}.

$$\mathcal{Z}_{\rm disc} = \sqrt{2[(s+b)\ln(1+s/b)-s]},$$
$$\mathcal{Z}_{\rm excl} = \sqrt{2[s-b\ln(1+s/b)]}. \quad (11)$$

In Fig. 6 and Fig. 7, the 2σ and 5σ lines are plotted as a function of κ^b and the VLQ-B mass M_B with the aforementioned three systematic error cases of δ=0, 5%, and 10%, for two fixed values of integrated luminosity 300 and 3000 fb^{-1}, respectively. We observe that our signals are rather robust against the systematic uncertainties on the background determination. For $\kappa_b = 0.5$ and $\delta = 0$, VLQ-B can be probed at the 5σ level with a mass of approximately 1950 (2300) GeV with the integral luminosity of 300 (3000) fb^{-1}, while the 2σ exclusion limits are approximately 2230 (2600) GeV with the integral luminosity of 300 (3000) fb^{-1}. When a realistic 5% systematic uncertainty is considered, the 5σ sensitivity decreases to 1800 (1900) GeV with the integral luminosity of 300 (3000) fb^{-1}. Meanwhile, the 2σ exclusion limits decreases to 2100 (2200) GeV with the integral luminosity of 300 (3000) fb^{-1}. Altogether, the higher systematic uncertainty of background can decrease the discovery capability and the excluded region.

We can now perform a comparison with other complementary studies for searches at the LHC run II involving a resonant VLQ-B. In Ref. [31], the authors use the same assumption on the parameters and design a dedicated search strategy for the $pp \to B \to bZ$ process via the $B \to Zb$ decay mode with $Z \to \ell^+\ell^-$ at $\sqrt{s} = 14$ TeV with an integrated luminosity of 300 fb^{-1}, and the numerical results show that for $\kappa_b = 0.5$, VLQ-B can be probed at the 5σ level with a mass of approximately 1620 GeV and an integral luminosity of 300 fb^{-1}. Using the model that includes a topless vectorlike doublet (B, Y), the author of [33] investigates the single production of a VLQ-B[1)], with the $B \to b + Z/H$ subsequent decay channel and the fully hadronic final states using a jet substructure at the 13 TeV LHC with an integrated luminosity of 300 fb^{-1}; a modest value of the chromomagnetic transition moments ($\kappa = 0.5$) enables the exclusion of $M \lesssim 1.8\,(2.2)$ TeV in the Z and H channels, respectively. Therefore, our analysis is competitive with the results of the existing literature and represents a complementary candidate to search for a possible VLQ-B.

Note that to avoid having to reject the overwhelming QCD multi-jet background, we do not consider other types of final events, such as the lepton+jets channel (where only one W boson decays leptonically and the other one decays hadronically) and all hadronic channel (where both of W bosons decay hadronically). Because

1) Note that this case using different assumptions on the parameters, the decay $B \to Wt$ is highly suppressed for the small mixing parameter $s_L \ll s_R$.

these channels are dependent on different tagging algorithms for the identification of boosted, hadronically decaying, heavy particles [80–82], i.e., to reconstruct the top quark, a new tagging technique, such as the heavy object tagger with variable R (HOTVR) [81] algorithm, can be used to identify jets from the collimated top quark decay, which is beyond the scope of this paper.

IV. CONCLUSION

Based on a simplified model to describe the interactions Bgb, we have investigated the potential for the 14 TeV LHC to discover the vectorlike bottom quark partner produced via its chromomagnetic moment interaction, $pp \to bg \to B$, with the subsequent decay channel $B \to tW$ and leptonic decay mode for the top quark and W boson. This production mechanism complements the traditional searches, which have relied on pair-production of vectorlike quark states or single production of these states through electroweak interactions. Our numerical results show that, with a benchmark coupling parameter $\kappa^b = 0.5$, the VLQ-B can be probed at the 5σ level with a mass of approximately 1950 (2300) GeV and an integral luminosity of 300 (3000) fb^{-1}. Meanwhile, the 2σ excluded region is of approximately 2230 (2600) GeV with an integral luminosity of 300 (3000) fb^{-1}. We expect that our analysis can represent a complementary candidate to search for such singlet VLQ-B quark at the upgraded LHC.

References

[1] A. De Simone, O. Matsedonskyi, R. Rattazzi *et al*., JHEP **04**, 004 (2013)
[2] N. Arkani-Hamed, A. G. Cohen, E. Katz *et al*., JHEP **0207**, 034 (2002)
[3] K. Agashe, R. Contino, and A. Pomarol, Nucl. Phys. B **719**, 165-187 (2005)
[4] H. J. He, T. M. P. Tait, and C. P. Yuan, Phys. Rev. D **62**, 011702 (2000)
[5] H. J. He, C. T. Hill, and T. M. P. Tait, Phys. Rev. D **65**, 055006 (2002)
[6] X. F. Wang, C. Du, and H. J. He, Phys. Lett. B **723**, 314-323 (2013)
[7] H. J. He and Z. Z. Xianyu, JCAP **10**, 019 (2014)
[8] J. A. Aguilar-Saavedra, R. Benbrik, S. Heinemeyer *et al*., Phys. Rev. D **88**, 094010 (2013)
[9] A. Atre, G. Azuelos, M. Carena *et al*., JHEP **08**, 080 (2011)
[10] M. Buchkremer, G. Cacciapaglia, A. Deandrea *et al*., Nucl. Phys. B **876**, 376 (2013)
[11] D. Barducci and L. Panizzi, JHEP **12**, 057 (2017)
[12] B. Fuks and H. S. Shao, Eur. Phys. J. C **77**(2), 135 (2017)
[13] S. Yang, J. Jiang, Q. S. Yan *et al*., JHEP **09**, 035 (2014)
[14] D. Liu, L. T. Wang, and K. P. Xie, JHEP **01**, 157 (2019)
[15] G. Cacciapaglia, A. Deandrea, N. Gaur *et al*., JHEP **11**, 055 (2018)
[16] J. A. Aguilar-Saavedra, J. Alonso-González, L. Merlo *et al*., Phys. Rev. D **101**(3), 035015 (2020)
[17] D. Wang, L. Wu, and M. Zhang, Phys. Rev. D **103**(11), 115017 (2021)
[18] Y. J. Zhang, L. Han, and Y. B. Liu, Phys. Lett. B **768**, 241-247 (2017)
[19] L. Han, Y. J. Zhang, and Y. B. Liu, Phys. Lett. B **771**, 106-112 (2017)
[20] Y. B. Liu, Nucl. Phys. B **923**, 312-323 (2017)
[21] Y. B. Liu and Y. Q. Li, Eur. Phys. J. C **77**(10), 654 (2017)
[22] Y. B. Liu and S. Moretti, Phys. Rev. D **100**(1), 015025 (2019)
[23] X. Y. Tian, L. F. Du, and Y. B. Liu, Nucl. Phys. B **965**, 115358 (2021)
[24] S. Moretti, D. O'Brien, L. Panizzi *et al*., Phys. Rev. D **96**(3), 035033 (2017)
[25] S. Moretti, D. O'Brien, L. Panizzi *et al*., Phys. Rev. D **96**(7), 075035 (2017)
[26] A. Carvalho, S. Moretti, D. O'Brien *et al*., Phys. Rev. D **98**(1), 015029 (2018)
[27] S. J. D. King, S. F. King, S. Moretti *et al*., JHEP **21**, 144 (2020)
[28] X. Qin and J.-F. Shen, Nucl. Phys. B **966**, 115388 (2021)
[29] L. Han and J. F. Shen, Eur. Phys. J. C **81**(5), 463 (2021)
[30] J. Z. Han, J. Yang, S. Xu *et al*., Phys. Rev. D **105**(1), 015005 (2022)
[31] X. Gong, C. X. Yue, and Y. C. Guo, Phys. Lett. B **793**, 175-180 (2019)
[32] X. Gong, C. X. Yue, H. M. Yu *et al*., Eur. Phys. J. C **80**, 876 (2020)
[33] D. Choudhury, K. Deka, and N. Kumar, Phys. Rev. D **104**(3), 035004 (2021)
[34] M. Aaboud *et al*. (ATLAS), Phys. Rev. D **98**(9), 092005 (2018)
[35] M. Aaboud *et al*. (ATLAS Collaboration), JHEP **1812**, 039 (2018)
[36] M. Aaboud *et al*. (ATLAS), Phys. Rev. D **98**(11), 112010 (2018)
[37] M. Aaboud *et al*. (ATLAS), JHEP **08**, 052 (2017)
[38] M. Aaboud *et al*. (ATLAS Collaboration), Phys. Rev. Lett. **121**, 211801 (2018)
[39] A. M. Sirunyan *et al*. (CMS), JHEP **11**, 085 (2017)
[40] A. M. Sirunyan *et al*. (CMS Collaboration), Phys. Rev. D **100**, 072001 (2019)
[41] A. M. Sirunyan *et al*. (CMS), JHEP **08**, 177 (2018)
[42] A. M. Sirunyan *et al*. (CMS), Phys. Rev. D **102**, 112004 (2020)
[43] A. M. Sirunyan *et al*. (CMS Collaboration), Phys. Rev. D **102 04**(2020), (1120)
[44] A. Buckley, J. M. Butterworth, L. Corpe *et al*., SciPost Phys. **9**(5), 069 (2020)
[45] M. Backovic, T. Flacke, J. H. Kim *et al*., JHEP **04**, 014 (2016)
[46] G. Cacciapaglia, A. Carvalho, A. Deandrea *et al*., Phys. Lett. B **793**, 206-211 (2019)
[47] A. Roy, N. Nikiforou, N. Castro *et al*., Phys. Rev. D **101**(11), 115027 (2020)
[48] X. Y. Tian, L. F. Du, and Y. B. Liu, Eur. Phys. J. C **81**(7), 594 (2021)
[49] A. Deandrea, T. Flacke, B. Fuks *et al*., JHEP **08**, 107 (2021)

[50] S. Bhattacharya, S. S. Chauhan, B. C. Choudhary *et al*., Phys. Rev. D **76**, 115017 (2007)
[51] S. Bhattacharya, S. S. Chauhan, B. C. Choudhary *et al*., Phys. Rev. D **80**, 015014 (2009)
[52] J. Nutter, R. Schwienhorst, D. G. E. Walker *et al*., Phys. Rev. D **86**, 094006 (2012)
[53] A. Belyaev, R. S. Chivukula, B. Fuks *et al*., Phys. Rev. D **104**(9), 095024 (2021)
[54] G. Aad *et al*. (ATLAS), Phys. Lett. B **721**, 171-189 (2013)
[55] V. Khachatryan *et al*. (CMS), JHEP **01**, 166 (2016)
[56] A. M. Sirunyan *et al*. (CMS), JHEP **12**, 106 (2021)
[57] A. Tumasyan *et al*. (CMS), JHEP **04**, 048 (2022), arXiv:2111.10216 [hep-ex]
[58] For a comprehensive review, H. J. He, Y. P. Kuang, and C. P. Yuan, arXiv: hep-ph/9704276
[59] H. J. He, Y. P. Kuang, and X. y. Li, Phys. Rev. Lett. **69**, 2619-2622 (1992)
[60] H. J. He, Y. P. Kuang, and X. y. Li, Phys. Rev. D **49**, 4842-4872 (1994)
[61] H. J. He, Y. P. Kuang, and C. P. Yuan, Phys. Rev. D **51**, 6463-6473 (1995)
[62] H. J. He, Y. P. Kuang, and C. P. Yuan, Phys. Rev. D **55**, 3038-3067 (1997)
[63] H. J. He and W. B. Kilgore, Phys. Rev. D **55**, 1515-1532 (1997)
[64] J. Alwall, R. Frederix, S. Frixione *et al*., JHEP **1407**, 079 (2014)
[65] R. D. Ball *et al*. (NNPDF Collaboration), JHEP **1504**, 040 (2015)
[66] V. Khachatryan *et al*. (CMS Collaboration), Eur. Phys. J. C **74**(9), 3060 (2014)
[67] M. Tanabashi *et al*. (Particle Data Group), Phys. Rev. D **98**, 030001 (2018)
[68] T. Sjöstrand, S. Ask, J. R. Christiansen *et al*., Comput. Phys. Commun. **191**, 159 (2015)
[69] M. Cacciari, G. P. Salam, and G. Soyez, Eur. Phys. J. C **72**, 1896 (2012)
[70] M. Cacciari, G. P. Salam, and G. Soyez, JHEP **0804**, 063 (2008)
[71] J. de Favereau *et al*. (DELPHES 3), JHEP **02**, 057 (2014)
[72] E. Conte, B. Fuks, and G. Serret, Comput. Phys. Commun. **184**, 222-256 (2013)
[73] R. Frederix and S. Frixione, JHEP **1212**, 061 (2012)
[74] M. Czakon, P. Fiedler, and A. Mitov, Phys. Rev. Lett. **110**, 252004 (2013)
[75] N. Kidonakis, Phys. Rev. D **96**(3), 034014 (2017)
[76] J. M. Campbell, R. K. Ellis, and C. Williams, JHEP **07**, 018 (2011)
[77] S. Catani, L. Cieri, G. Ferrera *et al*., Phys. Rev. Lett. **103**, 082001 (2009)
[78] E. Conte, B. Dumont, B. Fuks *et al*., Eur. Phys. J. C **74**(10), 3103 (2014)
[79] G. Cowan, K. Cranmer, E. Gross *et al.*, Eur. Phys. J. C **71**, 1554 (2011), [Erratum: Eur. Phys. J. C **73**, (2013) 2501]
[80] D. E. Kaplan, K. Rehermann, M. D. Schwartz *et al*., Phys. Rev. Lett. **101**, 142001 (2008)
[81] T. Lapsien, R. Kogler, and J. Haller, Eur. Phys. J. C **76**(11), 600 (2016)
[82] A. M. Sirunyan *et al*. (CMS), JINST **15**(06), P06005 (2020)